Scanning near-field ellipsometric microscope-imaging ellipsometry with a lateral resolution in nanometer range

P. Karageorgiev,[a] H. Orendi,[b] B. Stiller, and L. Brehmer
Physics of Condensed Matter, Institute of Physics, University of Potsdam, P.O. Box 60 15 53, 14415 Potsdam, Germany

(Received 12 March 2001; accepted for publication 16 July 2001)

An apertureless optical near-field scanning microscope system has been created by combining a commercially available atomic force microscope and an ellipsometer without any prior changes in design of the respective devices. In preliminary experiments, an optical resolution of about 20 nm ($\lambda/32$) has been achieved using the combined microscope. The intensity of the measured optical signal has been found to be a periodic function of the thickness of the sample. Moreover, the period of this function is dependent upon the local optical properties of the sample material. © *2001 American Institute of Physics.* [DOI: 10.1063/1.1403237]

Twenty years ago, visualization of the nanoworld could only have been regarded as an expensive and nearly impracticable undertaking. Today, with the introduction of elegant scanning probe techniques, beginning with tunnelling, then atomic force and near-field optical microscopes (SNOM), it has become an everyday reality for almost every group working in the field of materials science. Nonetheless, the potential of scanning microscopic methods has not yet been exhausted by far. This is especially obvious in the progress of the scanning optical microscopy, particularly in regard to the apertureless near-field devices. Since the early works of Wessel[1] and Fischer and Pohl,[2] we have been witnesses to the invention of the scanning plasmon,[2,3] light scattering (with a conventional metallic,[4,5] or laser-trapped particle[6] probe), fluorescence,[7,8] interferometric,[9] Raman,[10–12] and second-harmonic[13] microscopes.

The advantages of the apertureless near-field optical systems include: (a) higher resolution[9] (in the aperture SNOM, resolution is limited by the penetration depth of the light in the metal forming the aperture), (b) the possibility of using commercially available uniform probe tips, (c) the possibility of simultaneous study of the optical properties of the sample surface and its nonoptical properties with complete atomic force microscopy (AFM) power (topography, lateral force, force spectroscopy, electrostatic potential, etc.). In some cases, the scanning tip converts (e.g., by scattering of the evanescent field) the information contained in the local near field to a detectable far-field signal.[4–6] In other cases, the tip acts as a nanoobject, which concentrates and enhances the radiation from an external source in the tip–substrate gap. The matter of the sample, which is locally excited by the enhanced light, produces a detectable far-field signal.[10–13] By using apertureless SNOMs based on the local excitation, it is possible not only to characterize but also to modify the sample surface by generating local photochemical reactions.[14]

As a rule, in apertureless microscopy, the intensity of the detected optical signal is much lower than the intensity of the light which irradiates the sample. Therefore, a dark-field optical configuration is necessary. The difference in our proposed method to others is that we analyze the information contained in a beam reflected from the sample surface. This is done using a null ellipsometer. A similar approach, based on an interferometric detector has been proposed by Zenhausern *et al.*[9]

The attractiveness of optical reflection techniques such as ellipsometry or interferometry for detecting light–sample interaction which take place in the near field of the tip is based on their extremely high sensitivity for minute changes in interface properties. The method of imaging ellipsometry, which is, in a sense, a macroscopic analogue of our proposed method, allows the visualization of lateral inhomogeneities in the refractive index of thin films and also a quantification of these images. The transversal resolution (normal to the sample surface) is within the subnanometer range and of about 0.0001 in refractive index. This accuracy is quite remarkable since the probing light is usually within the visible range ($\lambda \sim 400-700$ nm).

However, as for any optical technique, the lateral resolution of the imaging ellipsometry is limited by a diffraction up to about half of the wavelength. The practically achieved value is not as good and under favorable conditions reaches approximately 2 μm (at $\lambda = 632.8$ nm). Moreover, due to the oblique angle of incidence, the true resolution differs in the x (in the plane of incidence) and the y directions (normal to the plane of incidence). The inclination of the illumination and of the direction of viewing, respectively, are also sources of problems related to the distortion of the image (a circle on the sample is imaged as an ellipse) and to the depth of field (only a narrow strip of the sample is in focus at any given time). The first problem can be solved by recalculating the image with respect to the angle of incidence. The depth of field can be improved by scanning the objective and reassembling the entire image from the strips recorded during scanning. A much more sophisticated approach relies on specially designed microscopic mirror objectives.[15,16] However, all these methods solve only the specific imaging problems

[a]Author to whom correspondence should be addressed; electronic mail: ppkara@rz.uni-potsdam.de
[b]Electronic mail: optrel@t-online.de

 © 2001 American Institute of Physics
Downloaded 21 Sep 2001 to 128.113.8.139. Redistribution subject to AIP license or copyright, see http://ojps.aip.org/aplo/aplcr.jsp

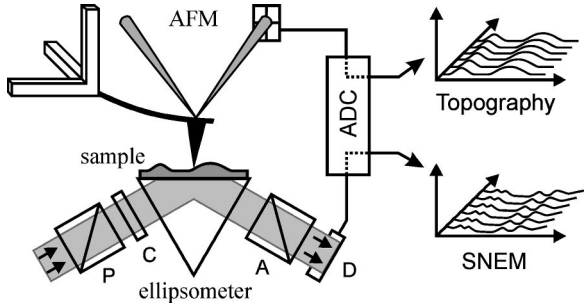

FIG. 1. Experimental setup of SNEM is shown. P denotes a polarizer, C—compensator, A—analyzer, and D—detector.

and do not lead to a significant improvement in lateral resolution.

In this letter, we introduce a microscope system which allows for imaging of inhomogeneities of optical properties of thin films with a lateral resolution within the nanometer range. The technique has no problems with depths of field and does not lead to the distortion of the images. Furthermore, unlike already presented apertureless SNOMs, the proposed system provides information about the local thickness of transparent films (note that the topography obtained using a conventional AFM is not equivalent to the film thickness). We have called this technique scanning near-field ellipsometric microscopy (SNEM).

The experimental setup consists of the combination of an AFM (''Explorer™,'' TopoMetrix Co., USA) with an ellipsometer (''Multiskop,'' Optrel GbR, Germany) as depicted in Fig. 1. Samples are thin, transparent polymer layers coated on glass plates. They are fixed on a prism with index matching fluid. The two-circle goniometer of the Multiskop is used in the vertical arrangement, both optical arms are rotated so that the probing light hits the sample from underside (see Fig. 1). The incident laser beam (He–Ne and $\lambda = 632.8\,\text{nm}$) passes through the prism and undergoes total internal reflection from the sample surface. The illuminated spot on the sample is ca. $0.5\,\text{mm}^2$. The ellipsometer is set in the null mode; i.e., the light intensity at the detector is minimized by the settings of the polarizers. This setting is not changed during the entire period of measurement. The detector of the Multiskop is connected to the electronic control unit of the AFM in order to record the optical signal simultaneously with the topographic data. The AFM is placed on the sample so that the tip is over the spot illuminated by the ellipsometer. During the measurement, the AFM operates in contact mode. By scanning the tip within the evanescent field, null-ellipsometry conditions are disturbed. The detector registers a change in the optical signal which is simultaneously displayed with the topography as a two-dimensional image.

Figure 2 presents two micrographs of the topography of a surface grating and the optically obtained images of the same areas. The grating was produced by illumination of an azobenzene-containing film with an interference pattern of two crossing laser beams (provided by Kulikovska). As a result, a periodic modulation of both the film topography and orientation of the azo-dye molecules takes place. The correlation and difference between conventional AFM and SNEM images are obvious. In addition to the surface grating, the SNEM image shows a superstructure formed by broad slop-

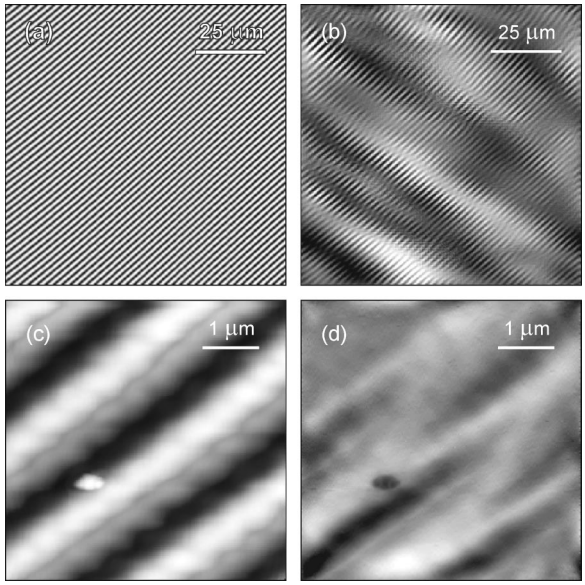

FIG. 2. Topography (a), (c) and SNEM (b), and (d) images of a surface grating are shown. Gary scale denotes 0–243 nm (a), 0–74 mV (b), 0–234 nm (c), and 0–34 mV (d).

ing waves [compare Figs. 2(a) and 2(b)]. Moreover, at close examination of the SNEM image [Fig. 2(b)] a 180° phase shift of the grating at valleys and ridges of the superstructure is visible. A $5 \times 5\ \mu$m scan of the phase-shift area is shown in Figs. 2(c) and 2(d). It is interesting to note that the structure of the particle is better resolved in a SNEM than in an AFM image.

Figure 3 provides information on the contrast mechanism of SNEM. The sample is a polycrystalline film of a thermotropic liquid crystal (provided by Janietz). The knoll-shape crystallites [Fig. 3(a)] are presented in the SNEM image [Fig. 3(b)] as inscribed contours. For example, the crystallite in the lower-right-hand side corner has a dark edge, then bright and dark contours follow and at the center are two small bright circles. The basic properties of the crystal-

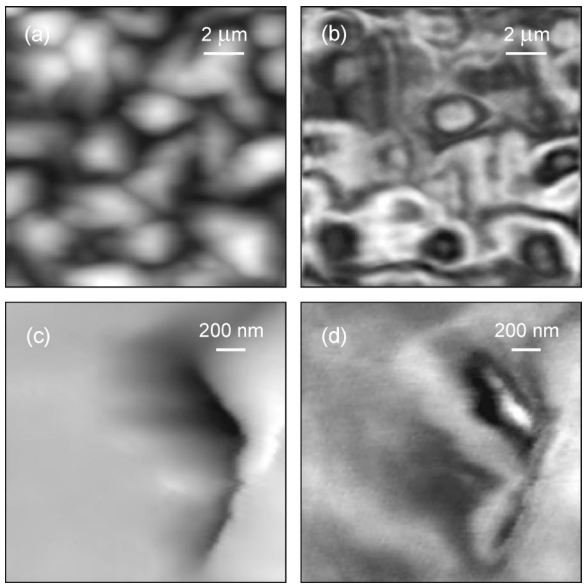

FIG. 3. Topography (a), (c) and SNEM (b), and (d) images of a polycrystalline film of a thermotropic liquid crystal are shown. Gary scale denotes 0–1.12 μm (a), 0–265 mV (b), 0–1.14 μm (c), and 0–42 mV (d).

Downloaded 21 Sep 2001 to 128.113.8.139. Redistribution subject to AIP license or copyright, see http://ojps.aip.org/aplo/aplcr.jsp

line state are the identical orientation and packing density of the molecules inside one monocrystal. Therefore, the periodic modulation of the SNEM signal by scanning within one crystallite can not be attributed to any change in the characteristics (e.g., refractive index or absorption coefficient) of the matter along this crystallite. Only the shape of the crystallite (i.e., the thickness) can cause the modulation of the optical signal. In order to test this, we have superimposed the SNEM image on the topography. It has been found that within crystallites the contours of the Fig. 3(b) reproduce approximately the isohypses of Fig. 3(a) (some deviations take place on the boundary between particles). This is similar to the conventional ellipsometric measurements, where the registered light intensity is a periodic function of the film phase thickness. The phase thickness depends on the complex refractive index, wavelength, film thickness, and angle of incidence.[17] Therefore, a different period (P_z) of the optical signal would be expected at different refractive indexes in particular. In fact, the period is not identical for all crystallites. For example, for the crystallite in the lower-right-hand side corner P_z is ~ 610 nm, and for the upper neighboring crystallite it is ~ 750 nm. This difference can arise due to differences in orientation of the strong-asymmetrical molecules in this crystallites (i.e., when the optical axes of the crystallites are not parallel). Figures 3(c) and 3(d) show a border between two crystallites. Objects distant ca. 20 nm from each other can be resolved on the optical image [Fig. 3(d)]. Some of them do not correlate with the topography [Fig. 3(c)].

Additional information concerning the contrast mechanism was obtained by using various tip materials. All presented images (Figs. 2 and 3) have been measured using a commercial platinum coated silicon conical tip (radius of curvature $r_c \sim 20$ nm). Measurements of the same samples with a gold coated tip (self made coating, $r_c \sim 40$ nm) have shown an approximately 40% lower amplitude of the optical signal. It was not possible to obtain optical images using uncoated silicon tips ($r_c \sim 20$ nm). It is known that a metallic tip converts the evanescent field into propagation waves more effectively than a dielectric one.[5] Therefore, it seems reasonable to assume that the optical contrast arises from interference of the propagating waves generated in the near field of the tip with the light reflected from the back surface of the film (a similar contrast mechanism has been discussed in Ref. 9). This could explain the sensitivity of our proposed near-field microscope to changes in film thickness up to several hundreds nanometers.

The presented images are obtained in the so-called constant gap-width mode[18] (the tip follows the topography). The z motion of the scanning probe in this operation mode usually causes a distortion of the optical image.[18–20] Our results show a modulation of the optical signal at z motions of the tip [Fig. 3(b)] and also without them [the superstructure in Fig. 2(b) and the lower-left-hand side half of Fig. 3(d)]. Therefore, measurements in constant height mode[18] should be performed for deeper understanding of the SNEM contrast mechanism.

In conclusion, we have demonstrated that by a combination of two devices, an atomic force microscope and an ellipsometer, it is possible to visualize optical inhomogeneities in thin transparent films at a resolution of about 20 nm. The experimental technique is simple. It can be used to measure the local refractive index, absorption, and thickness of thin films. Future studies are planned to obtain more information about the nature of the SNEM contrast mechanism.

The authors are grateful to J. Stumpe, O. Kulikovska, and D. Janietz (Institute of Thin-Film Technology and Microsensorics, Teltow) for providing us with test samples. They gratefully acknowledge the financial support of this work by the Deutsche Forschungsgemeinschaft.

[1] J. Wessel, J. Opt. Soc. Am. B **2**, 1538 (1985).
[2] U. C. Fischer and D. W. Pohl, Phys. Rev. Lett. **62**, 458 (1989).
[3] M. Specht, J. D. Pedarning, W. M. Heckl, and T. W. Hänsch, Phys. Rev. Lett. **68**, 476 (1992).
[4] H. K. Wickramasinghe and C. C. Williams, US Patent No. 4,947,034 (7 August 1990).
[5] Y. Inouye and S. Kawata, Opt. Lett. **19**, 159 (1994).
[6] S. Kawata, Y. Inouye, and T. Sugiura, Jpn. J. Appl. Phys., Part 2 **33**, L1725 (1994).
[7] A. Lewis and K. Liberman, Nature (London) **354**, 214 (1991).
[8] K. Liberman and A. Lewis, Ultramicroscopy **42**, 399 (1992).
[9] F. Zenhausern, Y. Martin, and H. K. Wickramasinghe, Science **269**, 1083 (1995).
[10] S. R. Quake, US Patent No. 6,002,471 (14 December 1999).
[11] R. M. Stöckle, Y. D. Suh, V. Deckert, and R. Zenobi, Chem. Phys. Lett. **318**, 131 (2000).
[12] N. Hayazawa, Y. Inouye, Z. Sekkat, and S. Kawata, Opt. Commun. **183**, 333 (2000).
[13] A. V. Zayats and V. Sandoghdar, Opt. Commun. **178**, 245 (2000).
[14] P. Karageorgiev, B. Stiller, D. Prescher, B. Dietzel, B. Schulz, and L. Brehmer, Langmuir **16**, 5515 (2000).
[15] C. Lheveder, S. Hénon, R. Mercier, G. Tissot, P. Fournet, and J. Meunier, Rev. Sci. Instrum. **69**, 1446 (1998).
[16] K. R. Neumaier, G. Elender, E. Sackmann, and R. Merkel, Europhys. Lett. **49**, 14 (2000).
[17] R. M. A. Azzam and N. M. Bashara, *Ellipsometry and Polarized Light* (North-Holland, Amsterdam, 1977), p. 284.
[18] B. Hecht, H. Bielefeldt, Y. Inouye, D. W. Pohl, and L. Novotny, J. Appl. Phys. **81**, 2492 (1997).
[19] S. I. Bozhevolnyi, I. I. Smolyaninov, and O. Keller, Appl. Opt. **34**, 3793 (1995).
[20] C. E. Jordan, S. J. Stranick, L. J. Richter, and R. R. Cavanagh, J. Appl. Phys. **86**, 2785 (1999).

Downloaded 21 Sep 2001 to 128.113.8.139. Redistribution subject to AIP license or copyright, see http://ojps.aip.org/aplo/aplcr.jsp